Journal of Applied Electrochemistry (2005) 35:285–291
DOI 10.1007/s10800-004-6770-y

Mass transfer studies at rotating cylinder electrodes of expanded metal

J.M. GRAU and J.M. BISANG*
*Programa de Electroquímica Aplicada e Ingeniería Electroquímica (PRELINE), Facultad de Ingeniería Química (UNL), Santiago del Estero 2829, S3000AOM Santa Fe, Argentina (*author for correspondance, fax: +54-342-4571162; e-mail: jbisang@fiqus.unl.edu.ar)*

Received 23 June 2004; Accepted in revised form 12 November 2004

Key words: electrochemical reactors, expanded metal, mass transfer, rotating cylinder electrode, three-dimensional electrodes

Abstract

Mass transfer has been studied at rotating cylinder electrodes of expanded metal using the reduction of ferricyanide as test reaction. The experimental data are well correlated by an empirical expression between the Sherwood number and the Reynolds number, both in terms of the hydraulic diameter as characteristic length, and including two additional dimensionless parameters in order to characterize the geometry of the expanded metal. Comparisons of the mass-transfer performance of the expanded metal electrodes with other three-dimensional structures are made.

List of symbols

a	constant in Equation 2
A	short mesh aperture (m)
A_s	specific surface area (m^{-1})
C	concentration (mol m^{-3} or mg l^{-1})
d	external cylinder diameter (m)
d_h	hydraulic diameter $= 4\varepsilon/A_s$ (m)
D	diffusion coefficient ($m^2\ s^{-1}$)
F	Faraday constant (C mol^{-1})
I_{lim}	limiting current (A)
k_m	mass-transfer coefficient (m s^{-1})
r_1	internal radius (m)
r_2	external radius (m)
$\bar{r}$	mean radius $= \sqrt{(r_1^2 + r_2^2)/2}(m)$
Re_d	Reynolds number in terms of d as characteristic length $= \omega\ r_2\ d\ /v$
Re	Reynolds number $= \omega\ r_2\ d_h/v$
Sc	Schmidt number $= v/D$
Sh_d	Sherwood number in terms of d as characteristic length $= k_m\ d/D$
Sh	Sherwood number $= k_m\ d_h/D$
v	velocity relative to the electrode (m s^{-1})
U	tangential velocity (m s^{-1})
V	absolute velocity (m s^{-1})
V_e	electrode volume (m^3)

Greek symbols

α	exponent of the Reynolds number in Equation 2
β	exponent of a dimensionless parameter in Equation 2
γ	angle between the strands of the expanded structure and the plane of the metal sheet (degree)
ε	porosity
κ	exponent of a dimensionless parameter in Equation 2
v	kinematic viscosity ($m^2\ s^{-1}$)
v_e	charge number of the electrode reaction
ω	rotation speed (rpm or s^{-1})

1. Introduction

The increasing requirements of legal limitations for environmental protection require the development of reliable and cost-effective processes for the treatment of effluents with small concentration of dangerous species. The electrochemical treatment of effluents can be efficiently performed with the use of the rotating cylinder electrode [1], where the good mass-transfer conditions are achieved by the movement of the electrode. Another strategy to obtain a high space time yield is the use of electrochemical reactors with three-dimensional electrodes [2] or the combination of the two above concepts: that is, a rotating three-dimensional electrode.

Thus, Kreysa and Brandner [3] investigated the behaviour of a rotating packed bed cell with radial flow of the electrolyte. The mass-transfer coefficients as a function of the rotating Reynolds number and the channel Reynolds number were determined using the reduction of ferricyanide on nickel plated steel spheres or silver deposition on graphite particles. Kreysa [4] reported a dependence of the Sherwood number upon both Reynolds number to the power 0.58.

Mass transport to rotating cylinder electrodes fabricated from reticulated vitreous carbon of different

porosities was studied by Nahlé et al. [5]. Using copper deposition as test reaction they found that the Sherwood number was dependent upon the Reynolds number, both defined in terms of the cylinder diameter, to the power 0.63. It was also concluded that the mass transfer coefficients are comparable to those at a smooth rotating disk electrode of the same diameter. Thus, the current enhancements are mainly due to the large electroactive area of the three-dimensional matrix.

Zhou and Chin [6] studied the mass transfer in an oblique rotating barrel as a function of various operating parameters, including the rotation speed, barrel tilt angle, percentage loading and percentage immersion. Bouzek et al. [7] reported mass transfer studies in a vertically moving particle bed electrochemical cell, the contribution of bed rotation was quantified and a suitable empirical correlation of the Sherwood criterion was proposed.

Expanded metal is a promising material for three-dimensional electrodes [8] due to its geometrical particularities and physical and mechanical properties. Thus, the feasibility of removal of cadmium [9] and tin [10] from dilute aqueous solutions was studied with the use of rotating cylinder electrodes of expanded metal. The metal removal has been efficiently performed and for cadmium deposition fractional conversion values twice as large were obtained using the rotating three-dimensional electrode than with a rotating plate, which can be attributed to three factors: (i) good mass-transfer conditions of the rotating cylinder electrode, (ii) high specific surface area of the expanded structures, and (iii) turbulence promoting action of the expanded metal depending on the orientation of the mesh with regard to the direction of motion of the electrode.

The aim of the present work is to quantify the mass-transfer to a rotating cylinder electrode of expanded metal and to compare the mass-transfer characteristics with similar rotating structures.

2. Experimental details

The experiments were performed in an undivided batch reactor (95 mm int. dia. and 140 mm high) thermostatted by a heating jacket. The working electrode was a rotating cylinder made by ordered packing of sheets of expanded metal of 316 stainless steel. Figure 1(a) depicts schematically the experimental arrangement. The lower part of the electrode was open but the upper part was joined to a Teflon sleeve in order to orientate the electrolyte flow through the sheet pack. A perforated Teflon disc, centrally positioned, was used as support of the three-dimensional electrode. The rotation speed was in the range 100–900 rpm, at higher values a pronounced vortex is formed and the incorporation of air bubbles in the solution was observed. The expanded sheets were arranged with the long diagonal parallel to the rotation axis. Thus, there were two possibilities for the orientation of the mesh with respect to the electrode rotation sense, sketched in Figure 1(b), where the velocity diagrams are also shown. For an electrolyte flowing through the rotating electrode, U is the velocity of a point on the electrode relative to the ground, v is the velocity of the electrolyte relative to the electrode and V is the absolute velocity of the electrolyte flowing through the electrode. The angle between the strands of the expanded structure and the plane of the metal sheet is called γ. It is noticeable that variant 1, acute γ, shows a higher value of absolute velocity than the variant 2.

Four types of mesh were used, named GF, CF, GG and MG; their geometrical characteristics, measured in the laboratory, are summarized in Table 1. Figure 1(c) shows the geometrical parameters which describe the geometry of the electrodes. The three-dimensional electrodes were arranged with a perfect superposition of the metal expanded sheets, which defines straight interconnected pores perpendicular to the rotation axis and diminishes the apparent thickness. A nickel plated stainless steel bolt passed through the bed thickness, pressing the electrode shaft and thus ensuring electric contact.

The test reaction was the electrochemical reduction of ferricyanide at nickel plated electrodes from solutions with $[K_3Fe(CN)_6] \cong 5 \times 10^{-4}$ M, $[K_4Fe(CN)_6] \cong 5 \times 10^{-2}$ M, in 1 M NaOH or 3 M NaOH as supporting electrolyte, while the reverse reaction occurs at the anode. Table 2 summarizes the composition and physicochemical properties of the solutions. The diffusion coefficient of ferricyanide in 3 M NaOH was calculated from the Stokes-Einstein parameter $D\mu/T = 2.25 \times 10^{-15}$ kg m s^{-2} K^{-1}, which was determined for 1 M NaOH as supporting electrolyte.

The three-dimensional electrode was plated with nickel. An adherent electrodeposit of nickel on the stainless steel expanded metal was obtained with the procedure suggested by Durney [11]: that is, (i) cathodic treatment in 1 M NaOH, (ii) use of the *Woods nickel strike* and (iii) nickel deposition from a conventional Watts type bath [12]. A smooth and compact deposit was obtained and no difference was observed between the inner and outer face of the three-dimensional electrode. Thus, the change in the electrode surface area due to nickel deposition is minimized. The cathode potential was swept from the open circuit potential (typically 100 mV vs SCE for 1 M NaOH and 125 mV for 3 M NaOH) to a value of −400 mV vs SCE and the current against potential curve was then recorded at a sweep rate of 1 mV s^{-1}. Samples of the solution were taken from the reactor after each experiment and the ferricyanide concentration was spectrophotometrically determined using a Perkin–Elmer model Lambda 20 double-beam UV–Vis Spectrophotometer with 10 mm glass absorption cells and as blank the supporting electrolyte was used. The measurements were performed at a wavelength of 430 nm, where it is possible to determine the ferricyanide concentration without interference by ferrocyanide. In a set of experiments the above procedure was repeated for five values of rotation speed in a given electrolyte. After two sets of experi-

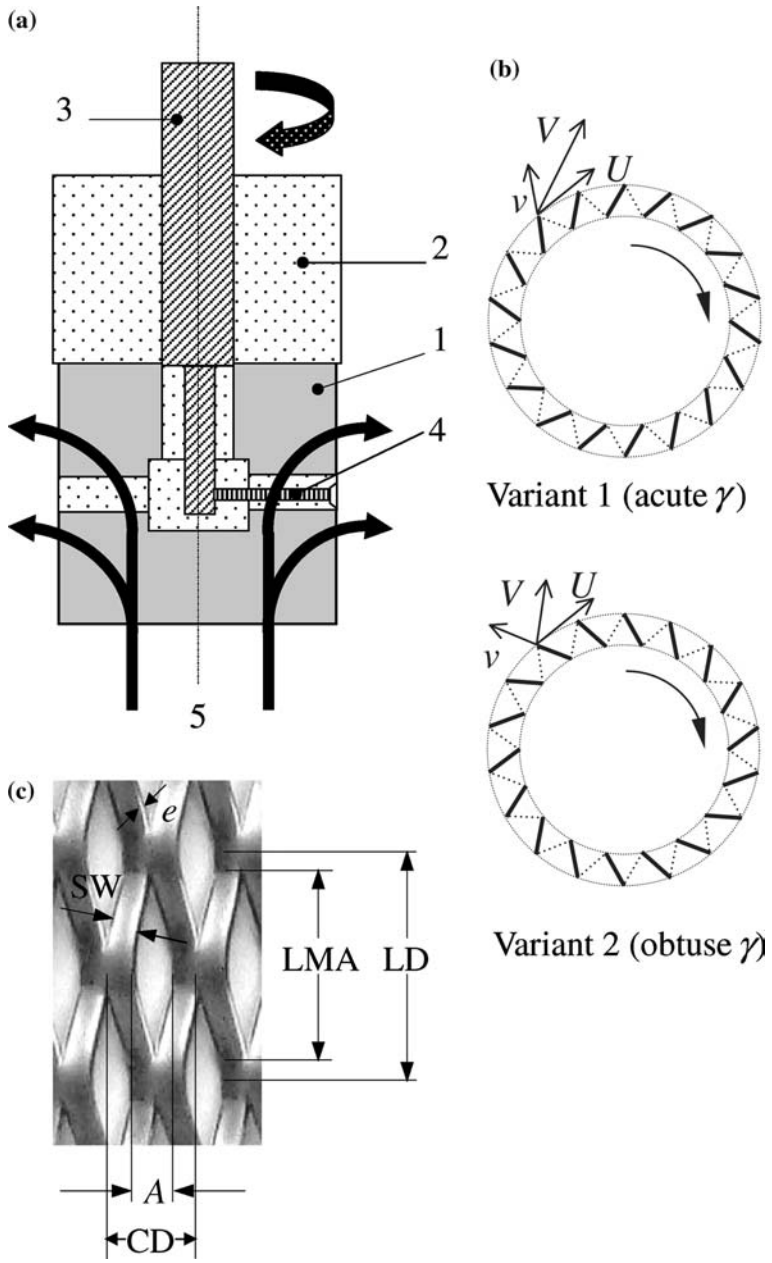

Fig. 1. (a) Schematic view of the working electrode. (1) working electrode, (2) Teflon sleeve, (3) electrode shaft, (4) electric contact and (5) electrolyte flow rate produced by the electrode rotation. (b) Orientations of the expanded metal structure. (c) View of the expanded metal with the characteristic parameters according to Table 1.

Table 1. Geometrical parameters of the electrodes

Characteristic parameters of the expanded metals	GF	CF	GG	MG
Long diagonal, LD/mm	10	6	10	16
Short diagonal, CD/mm	5	2.5	5.15	6.85
Long mesh aperture, LMA/mm	8	4.5	7	11
Short mesh aperture, A/mm	4	2	2.4	3
Thickness, e/mm	0.36	0.3	0.9	1
Apparent thickness, e_a (1 sheet)/mm	1.2	0.9	1.6	3
Apparent thickness (>1 sheet)/mm	0.95	0.7	1.55	2.5
Strand width, SW/mm	0.7	0.6	1.4	2
Surface area per unit volume of electrode, (1 sheet) A_s/m^{-1}	744	1628	1060	549
Surface area per unit volume of electrode, (>1 sheet) A_s/m^{-1}	940	2093	1094	659
Surface area per unit net area (1 sheet)	0.92	1.44	1.695	1.647
Porosity, ε (1 sheet)	0.907	0.847	0.674	0.797
Porosity, ε (>1 sheet)	0.882	0.803	0.663	0.756
Electrode length/mm	36.5	37	36.5	32

Table 2. Properties of electrolytes

Composition	$[K_3Fe(CN)_6] = 5 \times 10^{-4}$ M $[K_4Fe(CN)_6] = 5 \times 10^{-2}$ M [NaOH] = 1 M	$[K_3Fe(CN)_6] = 5 \times 10^{-4}$ M $[K_4Fe(CN)_6] = 5 \times 10^{-2}$ M [NaOH] = 3 M
Density/kg m^{-3}	1.05×10^3	1.12×10^3
Dynamic viscosity/kg m^{-1} s^{-1}	1.12×10^{-3}	1.55×10^{-3}
Kinematic viscosity/m^2 s^{-1}	1.07×10^{-6}	1.38×10^{-6}
Diffusion coefficient/m^2 s^{-1}	6.09×10^{-10}	4.40×10^{-10}
Sc	1757	3136

ments the nickel coating was stripped by acid immersion [13] and the electrode was plated with a fresh nickel surface. As counterelectrode a concentric helical platinum wire (1 mm dia. × 50 cm long) was used with an interelectrode gap of 11 mm.

As reference, a saturated calomel electrode was used and all potentials are referred to this electrode. The potential was controlled against the reference electrode connected to a Luggin capillary positioned at the middle of the outer face of the three-dimensional cathode. The experiments were performed at 30 °C and nitrogen was bubbled in the reactor for 1 h prior to the experiment in order to remove the dissolved oxygen.

In all the experiments the bed thickness of the three-dimensional electrodes was lower than the value given by Kreysa [14]. Thus, the whole bed is working under limiting current conditions and the mass-transfer coefficient was calculated from the limiting current and reactant concentration from the following equation

$$k_m = \frac{I_{lim}}{v_e F V_e A_s C} \tag{1}$$

3. Theoretical aspects

The mass-transfer at rotating three-dimensional electrodes can be studied taking into account the parameters k_m, U, ν, d_h and D as single variables and introducing $A/\bar{r}$ and $r_2/\bar{r}$ as additional geometric relations in order to take into account the characteristics of the three-dimensional electrode of expanded metal. The short mesh aperture, A, is a measure of the distance between consecutive turbulence promoters [15] and the external radius, r_2, takes into account the effect of the electrode size. Both A and r_2 were related to $\bar{r}$, which depends on the internal radius and on the electrode thickness. Performing a dimensional analysis results in the following dimensionless relationship

$$\frac{k_m d_h}{D} = a\left(\frac{U d_h}{\nu}\right)^{\alpha} Sc^{1/3} \left(\frac{r_2}{\bar{r}}\right)^{\beta} \left(\frac{A}{\bar{r}}\right)^{\kappa} \tag{2}$$

where the hydraulic diameter, taken as characteristic dimension, is given by

$$d_h = \frac{4\varepsilon}{A_s} \tag{3}$$

and

$$Sc = \frac{\nu}{D} \tag{4}$$

From hydrodynamic theory, the value of the Schmidt exponent was taken to be equal to 1/3.

Considering that the tangential velocity is

$$U = \omega r_2 \tag{5}$$

and comparing with the rotational Reynolds group introduced by Kreysa [4] then $\alpha = \beta$. Therefore, Equation 2 is simplified to

$$\frac{k_m d_h}{D} = a\left(\frac{\omega r_2 d_h}{\nu} \times \frac{r_2}{\bar{r}}\right)^{\alpha} Sc^{1/3} \left(\frac{A}{\bar{r}}\right)^{\kappa} \tag{6}$$

Defining a rotational Reynolds number as

$$Re = \frac{\omega r_2 d_h}{\nu} \tag{7}$$

gives

$$Sh = a\left(Re \times \frac{r_2}{\bar{r}}\right)^{\alpha} Sc^{1/3} \left(\frac{A}{\bar{r}}\right)^{\kappa} \tag{8}$$

4. Results

Figure 2 shows double logarithmic plots of Equation 8, where the Sherwood and Reynolds numbers are defined in terms of the hydraulic diameter as characteristic length. Table 3 reports the correlation parameters according to the least squares method applied to each set of experimental points. α is close to 0.6 in all cases in accordance with previous studies performed with rotating three-dimensional electrodes. Otherwise, for the GF and CF types of mesh, the electrodes with an acute orientation, variant 1, show values of mass-transfers lightly higher than those with an obtuse orientation.

The constants a and κ in Equation 8 may be determined from a double logarithmic plot of $a \times (A/\bar{r})^{\kappa}$ against $A/\bar{r}$. The slope of the correlation line gives $\kappa = 0.94$. Figure 3 shows that the data of the present study fit the equation:

$$Sh = 1.356\left(Re \times \frac{r_2}{\bar{r}}\right)^{0.63} Sc^{1/3} \left(\frac{A}{\bar{r}}\right)^{0.94} \tag{9}$$

with a correlation coefficient of 0.97 and 0.13 as standard deviation. Attemps to obtain an empirical

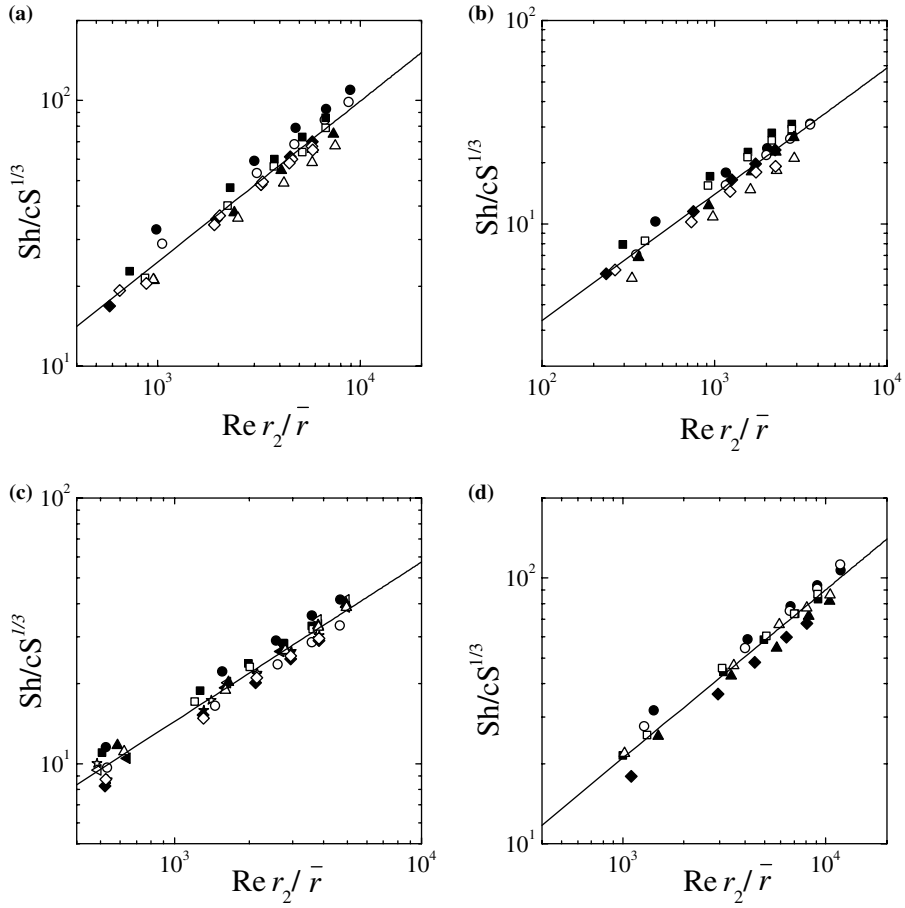

Fig. 2. Sherwood-Reynolds correlation for the four types of mesh. (a) GF meshes, (b) CF meshes, (c) GG meshes and (d) MG meshes. For (a) and (b): (●): 1 mesh, 1 M NaOH, acute γ. (○):1 mesh, 1 M NaOH, obtuse γ. (■):1 mesh, 3 M NaOH, acute γ. (□) : 1 mesh, 3 M NaOH, obtuse γ. (▲): 3 meshes, 1 M NaOH, acute γ. (△): 3 meshes, 1 M NaOH, obtuse γ. (♦): 3 meshes, 3 M NaOH, acute γ. (◇): 3 meshes, 3 M NaOH, obtuse γ. For (c) and (d): (●): 1 mesh, 1 M NaOH, acute γ. (○):1 mesh, 1 M NaOH, obtuse γ. (■):1 mesh, 3 M NaOH, acute γ. (□) : 1 mesh, 3 M NaOH, obtuse γ. (▲): 2 meshes, 1 M NaOH, acute γ. (△): 2 meshes, 1 M NaOH, obtuse γ. (♦): 2 meshes, 3 M NaOH, acute γ. (◇): 2 meshes, 3 M NaOH, obtuse γ. For (c): (◀): 2 meshes, 1 M NaOH, inner acute-outer obtuse. (◁): 2 meshes, 1 M NaOH, inner obtuse -outer acute. (★):2 meshes: 3 M NaOH, inner acute-outer obtuse. (☆): 2 meshes: 3 M NaOH, inner obtuse-outer acute.

Table 3. Summary of correlation parameters

Mesh type	Orientation	$a \times (A/\bar{r})^{\kappa}$	α	Correlation coefficient	Standard deviation
GF	Acute γ	0.371	0.61	0.97	0.13
	Obtuse γ	0.376	0.60	0.98	0.10
CF	Acute γ	0.214	0.61	0.98	0.11
	Obtuse γ	0.172	0.63	0.96	0.15
GG	Acute γ	0.254	0.59	0.97	0.11
	Obtuse γ	0.241	0.59	0.99	0.06
	Composite γ	0.199	0.62	0.99	0.06
MG	Acute γ	0.258	0.63	0.97	0.12
	Obtuse γ	0.219	0.65	0.96	0.16

expression in terms of other geometrical parameters did not produce a better correlation.

5. Comparison with previous studies

To provide comparison with existing mass-transfer data at rotating cylinder electrodes, Table 4 summarizes

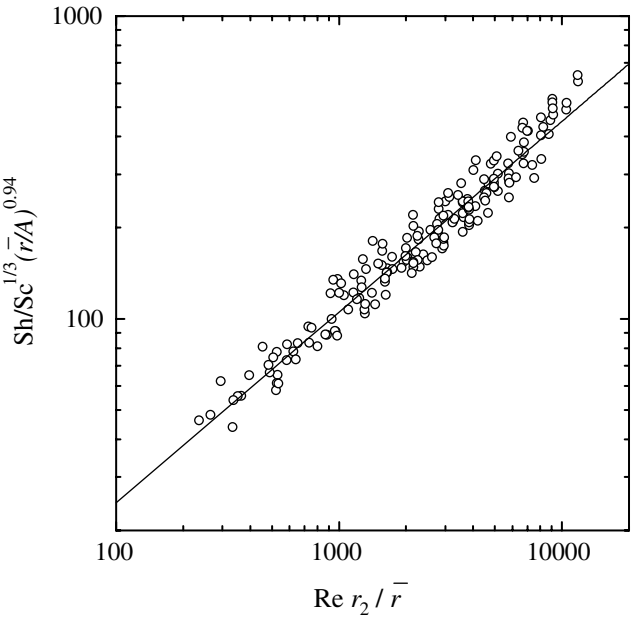

Fig. 3. Mass-transfer data against Reynolds number for the four types of mesh.

Table 4. Summary of mass-transfer correlations under the following form: $Sh_d = a Re_d^{\alpha} Sc^{c} \times factor$

	a	α	c	Factor	Validity range
Eisenberg et al. [16]	0.0791	0.7	0.356	1	$112 < Re_d < 1.62 \times 10^5$ $2230 < Sc < 3650$
Holland [17]	0.0791	0.92	0.356	1	$8 \times 10^4 < Re_d < 8.7 \times 10^6$
Nahlé et al. [5]	0.44	0.63	1/3	1	$10^3 < Re_d < 10^4$ $Sc = 2388$
Kreysa* [4]	0.454	0.58	1/3	$\left(\frac{d_h}{2\varepsilon\bar{r}}\right)^{0.58} \times \left(\frac{d_h}{r_2 - r_1}\right)^{1.116} \times \frac{d}{d_h}$	$Re_d < 5 \times 10^5$ $Sc = 1670$
Eq. 9, this study	1.356	0.63	1/3	$\left(\frac{d_h}{2\bar{r}}\right)^{0.63} \times \left(\frac{d}{d_h}\right) \times \left(\frac{A}{\bar{r}}\right)^{0.94}$	$4.8 \times 10^3 < Re_d < 9.2 \times 10^4$ $1757 < Sc < 3136$

(*) for channel Reynolds number zero, with $d_h = \varepsilon\, d_p/(1-\varepsilon)$, being d_p particle diameter.

some mass-transfer correlations. The equation of Eisenberg et al. [16], valid for smooth electrodes, and the Holland expression [17], valid for metal powder deposition, are included in Table 4. These correlations are given because they represent two limiting behaviours of mass-transfer at rotating cylinder electrodes. Further dimensionless equations as a function of the roughness factor are summarized by Gabe et al. [18], where it can be observed that all the data lie between the two above correlations. In Table 4 for the expression proposed by Kreysa [4] and for Equation 9 of this study a transformation factor is given, which allows the correlations to be rewritten in terms of the Sherwood and Reynolds numbers according to Eisenberg et al. Figure 4 compares the results for a Schmidt number of 2000. A value of 1.05 was adopted for the transformation factor in the Kreysa equation and 0.42 for the correlation of this study, which represents a mean value for the geometrical arrays. The validity range of each correlation is also given. The experimental data are about three times higher than the values expected for smooth electrodes. Thus, the expanded metal strongly enhances the mass-transfer behaviour. Likewise, the three correlations valid for three-dimensional rotating cylinder electrodes are very close in spite of the different materials used for the electrodes.

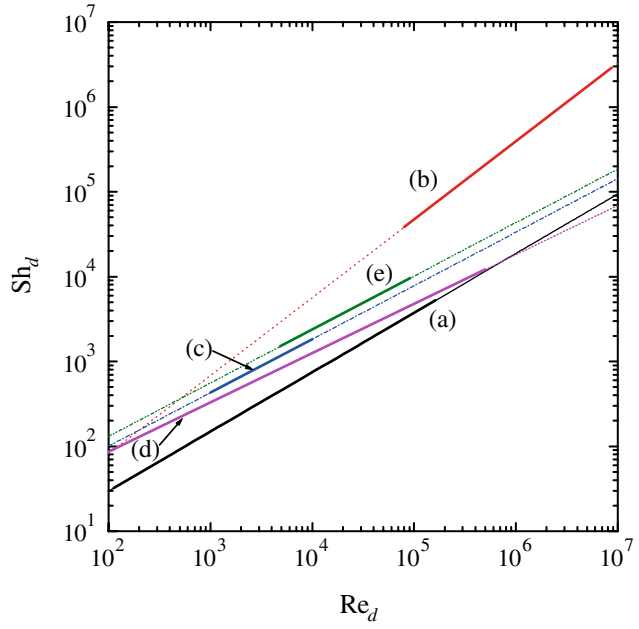

Fig. 4. Comparison of mass-transfer correlations for rotating cylinder electrodes. Sherwood and Reynolds number are given in terms of the diameter of the rotating electrode as characteristic length, according to Table 4. Thick lines: validity range of the expressions. Thin lines: extrapolation of the mass-transfer correlations. Sc = 2000. (a): Eisenberg et al. [16]. (b): Holland [17]. (c): Nahlé et al. [5]. (d): Kreysa [4]. (e): This study.

6. Conclusions

The experimental study of mass-transfer at rotating cylinder electrodes of expanded metal showed that mass transfer coefficients are about three times higher than those obtained with smooth rotating cylinder electrodes in the same conditions. The enhancement in the mass-transfer conditions can be attributed to the turbulence promoting action of the expanded structure.

The mass-transfer at rotating electrodes of expanded metal is influenced by the geometric parameters of the expanded metal. Nevertheless, the experimental results are well correlated by a single equation when two parameters characterizing the geometry of the expanded metal ($A/\bar{r}$ and $r_2/\bar{r}$) are included.

Acknowledgements

This work was supported by the Agencia Nacional de Promoción Científica y Tecnológica (ANPCyT), Consejo Nacional de Investigaciones Científicas y Técnicas (CONICET) and Universidad Nacional del Litoral (UNL) of Argentina. The authors are grateful to Model Chemical Laboratory (Facultad de Ingeniería Química-UNL) for the facilities to perform the spectrophotometric analysis.

References

1. F.C. Walsh, *in* D. Genders and N. Weinberg (Eds), 'Electrochemistry for a Cleaner Environment', (The Electrosynthesis Company, New York, 1992), pp. 101–159.

2. D. Pletcher and F.C. Walsh, *in* D. Genders and N. Weinberg (Eds), 'Electrochemistry for a Cleaner Environment', (The Electrosynthesis Company, New York, 1992), pp. 51–100.
3. G. Kreysa and R. Brandner, *in* 'Modern Concepts in Electrochemical Reactor Design', Extended Abstracts of the 31st ISE Meeting, Venice, Italy, **2** (1980) H8.
4. G. Kreysa, *Chem. Ing. Tech.* **55** (1983) 23 (In German).
5. A.H. Nahlé, G.W. Reade and F.C. Walsh, *J. Appl. Electrochem.* **25** (1995) 450.
6. C.D. Zhou and D.T. Chin, *J. Electrochem. Soc.* **142** (1995) 1993.
7. K. Bouzek, R. Chmelíková, M. Paidar and H. Bergmann, *J. Appl. Electrochem.* **33** (2003) 205.
8. F. Leroux and F. Coeuret, *Electrochim. Acta* **30** (1985) 159 and 167.
9. J.M. Grau and J.M. Bisang, *J. Chem. Technol. Biotechnol.* **78** (2003) 1032.
10. J.C. Bazan and J.M. Bisang, *J. Appl. Electrochem.* **34** (2004) 501.
11. L.J. Durney, *in* 'Ullmann's Encyclopedia of Industrial Chemistry', (VCH Verlagsgesellschaft, Weinheim, 1987), p.142.
12. H. Brown and B.B. Knapp , *in* F.A. Lowenheim (Ed), 'Modern Electroplating', 3rd edn (John Wiley & Sons, New York, 1974), Ch. 12, p. 292.
13. E.B. Saubestre, *in* F.A. Lowenheim (Ed), 'Modern Electroplating', 3rd edn (John Wiley & Sons, New York, 1974), Ch. 32, p. 762.
14. G. Kreysa, *DECHEMA Monographs* **94** (1983) 123 (in German).
15. S. Piovano and U. Böhm, *J. Appl. Electrochem.* **17** (1987) 123.
16. M. Eisenberg, C.W. Tobias and C.R. Wilke, *J. Electrochem. Soc.* **101** (1954) 306.
17. F.S. Holland, *Chem. and Ind.* **July** (1978) 453.
18. D.R. Gabe, G.D. Wilcox, J. Gonzalez-Garcia and F.C. Walsh, *J. Appl. Electrochem.* **28** (1998) 759.